A. LISIECKI*

WELDING OF THERMOMECHANICALLY ROLLED FINE-GRAIN STEEL BY DIFFERENT TYPES OF LASERS

SPAWANIE STALI DROBNOZIARNISTEJ WALCOWANEJ TERMOMECHANICZNIE LASERAMI RÓŻNEGO TYPU

The autogenous laser welding of 2.5 mm thick butt joints of thermomechanically rolled fine-grain steel grade S420MC was investigated. Butt joints were laser welded by the Yb:YAG Disk laser, emitted a circular laser beam with spot diameter of 200 μm at 1.03 μm wavelength, and also by the high power direct diode laser, emitted a rectangular beam with dimension of 1.8×6.8 mm at 808 nm wavelength. Different welding modes were identified for the lasers applied. The conduction welding mode was observed in whole of the diode laser welding parameters. While high quality joints, without any internal defects and characterized with satisfactory mechanical performance were produced in a wide range of parameters. The butt joints produced by Disk laser were welded at keyhole mode. In this case a slight tendency to weld porosity was found.

Keywords: laser, welding, keyhole, thermomechanically rolled, fine-grain steel

W artykule przedstawiono wyniki badań procesu spawania laserowego bez materiału dodatkowego złączy doczołowych ze stali drobnoziarnistej walcowanej termomechanicznie S420MC. Złącza doczołowe spawano laserowe za pomocą lasera dyskowego Yb:YAG, który emituje wiązkę laserową o przekroju kołowym i średnicy ogniska 200 μm przy długości fali promieniowania laserowego 1.03 μm, jak również za pomocą lasera diodowego dużej mocy o prostokątnym kształcie ogniska i długości fali 808 nm. Badania wykazały, że mechanizmy i techniki spawania zastosowanymi laserami są odmienne. W przypadku lasera diodowego w całym zakresie parametrów spawanie odbywało się z utworzeniem jeziorka spoiny. Złącza próbne spawane w szerokim zakresie parametrów charakteryzowały się wysoką jakością, brakiem wad wewnętrznych i wysokimi właściwościami mechanicznymi. Z kolei zastosowanie lasera dyskowego spowodowało, że złącza doczołowe były spawane z utworzeniem kanału parowego, tzw. oczka spoiny. W tym przypadku stwierdzono jednak nieznaczną skłonność do porowatości spoin.

1. Introduction

Modern high strength steels (HSS) are increasingly used in the industry for producing of welded structures [1-3]. The reason for that is to reduce the weight and increase the strength of structures. In order to take advantage of these steels, welding technology must provide high performance of joints at the level comparable to the base material [1-6]. One grade of such modern steels are microalloyed structural steels manufactured during thermomechanically rolling and characterized by fine-grains, and high yield point up to 700 MPa [2]. Steels of this type have low carbon equivalent, low content of alloying elements, so-called microelements, at precisely set proportions. Mechanical properties of this type of steels depend on the plastic deformation degree, temperatures of rolling and cooling rate after the rolling process [1,3,9-15]. They are considered to be well weldable due to their low value of carbon equivalent and also low content of contaminations, mainly sulphur and phosphorus [1,3-13]. Manufacturers of the microalloyed thermomechanically rolled steels provide just a little information about the welding procedures, limiting them only to conventional arc welding methods, mainly to gas metal arc welding (GMAW) or submerged metal arc welding (SMAW) [1]. Additionally the influence of welding process on the impact strength of these steel grades joints is completely omitted. Górka J. and also other researchers have shown that in the case of welding of the fine-grained and especially ultra-fine grained steels by conventional arc welding methods such as GMA or SMAW the heat input has a significant influence on the mechanical performance of weld joint [6]. Many researches indicate that due to excessive heat input grain coarsening in the heat affected zone (HAZ) may cause the performance mismatch between HAZ and the base metal (BM) decreasing the mechanical performance of welded joint dramatically [2-6]. To counteract this phenomenon it is recommended to keep the heat input low. Węgrzyn T. et al. propose an innovative technology of micro-jet cooling in GMA welding, which allows to increase the cooling rate, and thus increase the percentage of acicular ferrite in the weld metal [16-18]. Other researches recommend hybrid technologies, which combine arc and laser beam, and provide relatively high speeds of welding, compared to conventional arc processes. But even in this case an excessive heat input may significantly decrease the mechanical performance of joints, as shown Ming Gao et al. [4]. Nowa-

* SILESIAN UNIVERSITY OF TECHNOLOGY, WELDING DEPARTMENT, 18A KONARSKIEGO STR., 44-100 GLIWICE, POLAND

1626

days laser welding technologies are also increasingly being used in the industry because of many advantages [18-25]. The mechanism of laser welding is quite different compared to the arc and also hybrid welding processes [4,8,21-27]. Moreover the laser welding mode depends on the laser beam properties, thus the laser type. Grajcar A. et al. were investigated the keyhole welding of thermomechanically rolled steel sheets 2.0 mm thick, and they report that the dynamic thermal cycle of laser welding have most significant impact on the structural changes and microhardness of joint [25]. There is no report so far on the effect of laser welding by different lasers and different welding modes on the performance of butt joints of thermomechanically rolled steel sheets. Therefore, the study of laser welding of S420MC steel sheets by high power direct diode laser and Disk laser were performed.

2. Experimental procedure

The steel sheets used in the study were thermomechanically rolled, high yield strength steel for cold forming S420MC (according to EN 10149, and 060XLK according to ASTM) with a thickness of 2.5 mm, Table 1,2. Two types of lasers with different characteristic were used for autogenous welding of test joints, Fig 1. The high power direct diode laser (HPDDL) was characterized by a rectangular laser beam spot size 1.8×6.8 mm, and emitted in continuous wave at 808 nm, with maximum output power 2.2 kW. The laser head (including laser generator) was mounted above the sheets to be welded, and the laser beam was directly delivered into the weld region (weld pool). The rectangular laser beam spot was focused on the top surface and set along the welding direction. While the Disk laser used for investigations emits a circular laser beam at 1.03 μm wave length, characterized by beam parameter product (BPP) 8.0 mm·mrad. The maximum output power of the Disk laser is 3.3 kW. The laser beam was delivered into the focusing optics via fiber core of 200 μm in

diameter and 20 meters long. The laser welding head (focusing optics) was equipped with a 200 mm collimator lens and a 200 mm focusing lens. With this configuration of laser optics, the nominal beam spot diameter was 200 μm. Specimens for welding tests were cut from a steel sheet into pieces in dimension of 100.0×100.0 mm by means of industrial 2D cutting machine with CO_2 laser. Prior to welding test the specimens were sandblasted and additionally the edges to be welded were cleaned by acetone. Next the specimens were placed on the fixture device in such a way to ensure contact of the edges to be welded (I-joint type), then tightly clamped to eliminate any distortion or displacement during laser welding, Fig. 1. The weld pool was protected by argon flow at 12.0÷15.0 l/min via a cylindrical nozzle set at an angle 40÷45° to the steel sheet surface, in front of the weld pool. The test welded joints were investigated by visual inspection, metallographic examinations, including macro and microstructure analysis, micro-hardness distribution across the joints and mechanical tests such as tensile tests and bending tests. In order to compare the thermal conditions and cooling rates a thermal cycle were measured on top surfaces of joints by a pyrometer with measurement area of 0.3 mm. Result of the test and analysis are given on the Fig. 2 to 9, and in the Table 3 to 5.
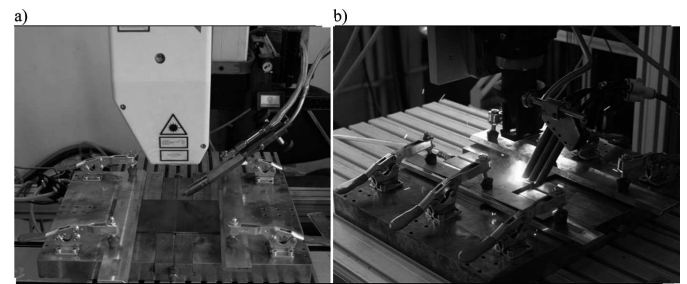

Fig. 1. Experimental setup for autogenous laser welding of butt joints equipped with : a) HPDDL ROFIN DL 020, and b) Disk laser TRUMPF TruDisk 3302

TABLE 1

Chemical composition of the investigated steel, Table 2

	Content % wt.								
	C	Mn	Si	V	Nb	Ti	Al	P	S
according to EN-10149-3	max 0.12	max 1.60	max 0.5	max 0.2*	max 0.09	max 0.15*	max 0.015	max 0.025	max 0.015
by certificate**	0.05	0.99	0.02	0.004	0.049	–	0.031	0.008	0.006

*Nb+Ti+V ⩽ 0.22%, ** certificate of Ruukki Company

TABLE 2

Mechanical properties of the investigated steel, Table 1

Nominal thickness, mm	<3	⩾ 3
Total elongation, A80 or A5, %	A80 16	A5 19
Minimum yield strength ReH, MPa	⩾ 420	
Tensile strength Rm, MPa	480÷620	
Notch impact energy at -20°C, KV, J	⩾ 40	
Notch impact energy at -40°C, KV, J	⩾ 27	

Parameters of butt joints welding of the 2.5 mm thick S420MC steel sheets using the HPDDL laser beam, Fig. 1 to 7

Test joint type	Laser power W	Welding speed mm/min	Heat input J/mm	Width of the weld face mm	Width of the weld root mm	Bend angle °	Tensile strength MPa
A	2200	350	380	2.9	0.5	180	568
B	2200	300	440	3.4	3.0	180	573
C	2200	200	660	3.5	3.4	180	575

Remarks: other parameters of laser welding : wavelength of laser radiation: 808 nm, focal length: 82.0 mm, dimensions of laser beam spot: 1.8×6.8 mm, diameter of the gas shielding nozzle: 12.0 mm, shielding gas: Ar (purity 99.999%), gas feed rate on the top surface (face of weld): 12.0 l/min and from root 3.0 l/min

3. Results and discussion

The autogenous laser welding tests of the S420MC steel sheets with the HPDDL laser beam have shown that, in a case of the butt joints 2.5 mm thick, the minimum heat input required for full penetration is 380 J/mm, at maximum power 2.2 kW and welding speed 350 mm/min, Fig. 2,3. Increase of the heat input to 660 J/mm, as a result of reducing the welding speed to 200 mm/min, leads to increase the root width to 3.4 mm and also increase of the weld face width to 3.5 mm, and the HAZ width is about 2.0 mm, Fig. 3, Table 3. Further increase of heat input leads to burn-through of the weld metal. Fusion zones showed on the macrographs of the test butt joints welded by HPDDL laser have a triangular shape at lower heat input (about 400 J/mm) or columnar shape at high heat input (660 J/mm), Fig. 2,3. The depth/width ratio of fusion zones is in a range from 0.7 to 0.9, similarly like in a case of conventional arc welding processes, e.g. TIG or even PTA welding. Thus the shape and geometry of fusion zones indicate clearly that all of the butt joint were laser welded at conduction welding mode. The reason for this is a relatively large area of the HPDDL laser beam spot with dimensions of 1.8×6.8 mm, and therefore even at maximum laser power of 2.2 kW the power density reaches just $3.25 \cdot 10^4$ W/cm^2, insufficient to form a key hole. Visual inspection, as well as the macro and microscope observations of the test joints shoved that the weld geometry is accepted. The surfaces of weld face and root are smooth and flat or with a little reinforcement (slightly convex), and without any internal defect, such as porosity, cracks or inclusions, Fig. 2,3.

Fig. 3. Macrostructure of the butt joints produced by: a) HPDDL at 660 J/mm ($t_{8/5}$ = 22 s), b) Disk laser at 38 J/mm ($t_{8/5}$ = 0.16 s)

The microstructure of the base metal of S420MC steel consists of fine-grained ferrite and retained austenite with average grains size about 10÷12 μm, Fig. 4. The microstructure of weld metal clearly depends on the heat input of HPDDL welding and it consists of different types of ferrite such as polygonal ferrite (α_{pf}), widmanstatten ferrite (α_{wf}), allotriomorphic ferrite (α_{af}), acicular ferrite (α_{ac}), Fig. 5. Additionally it can be noticed that the microstructure is similar to that of arc welding. Fusion zone of the butt joint produced at heat input of 380 J/mm is characterized by relatively high amount of acicular ferrite (needle shaped crystallites of grains) about 25%, and low amount of polygonal ferrite with average grain size of 20÷30 μm, Fig. 5. Increased heat input of 660 J/mm caused significant decrease of acicular ferrite in the fusion zone to about 15%, and simultaneous increase of the polygonal ferrite, additionally characterized by higher grain size of about 52 μm, Fig. 5.

Fig. 4. Microstructure of base metal of the S420MC steel sheet 2.5 mm thick (ferrite + retained austenite, grain size 10÷12 μm)
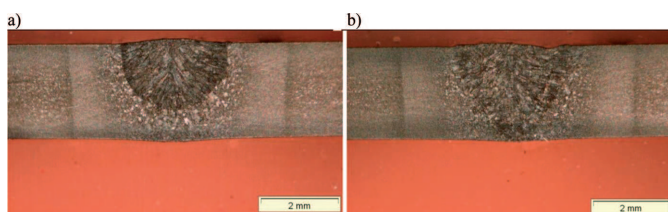

Fig. 2. Macrostructure of the bead-on-plate welds produced by the HPDDL laser on the 2.5 mm thick sheet of S420MC steel at heat input of: a) 330 J/mm, (2.2 kW, 400 mm/min), b) 380 J/mm (2.2 kW, 350 mm/min)
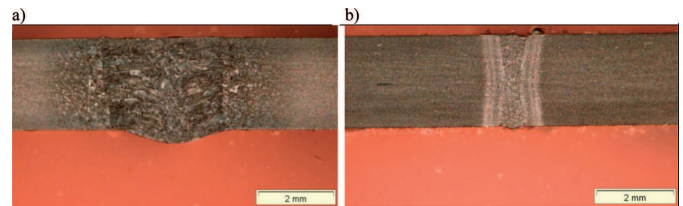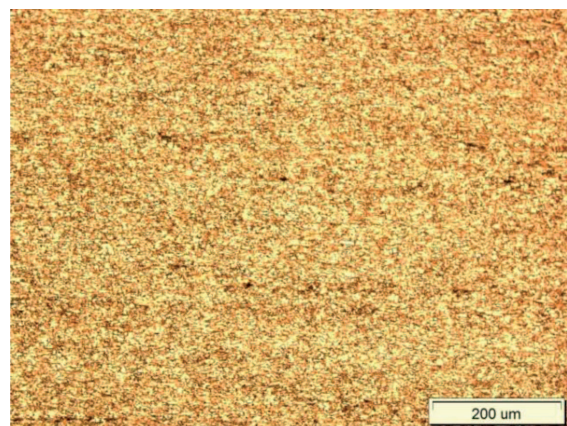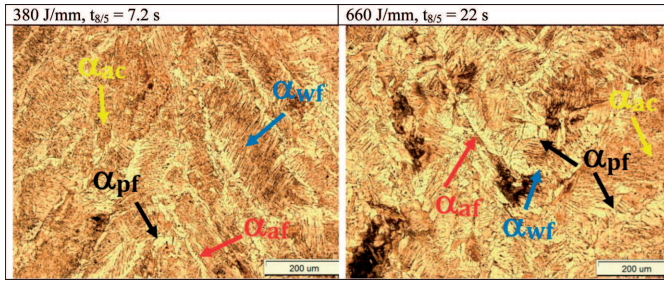
Fig. 5. Weld metal microstructure of the butt joints produced by HPDDL, Table 3,4; α_{pf} – polygonal ferrite, α_{wf} – widmanstatten ferrite, α_{af} – allotriomorphic ferrite, α_{ac} – acicular ferrite

The heat affected zone (HAZ) of butt joints is recrystallized with the structure, grain size and width dependent on the heat input, therefore thermal cycle of laser welding and cooling time between 800 and 500°C ($t_{8/5}$), Fig. 6, Table 4. The thermal cycles and therefore cooling times were measured on the top surface of welded joints by pyrometer. Additionally the cooling times between 800 and 500°C were calculated for different heat inputs of laser welding by means of the equation commonly used in a case of arc welding, but adopted for the laser beam welding conditions [2].

$$T_{8/5} = (4300 - 4.3 \cdot T_0) \cdot 10^5 \cdot \frac{k^2 \cdot E^2}{d^2} \cdot \left[\left(\frac{1}{500 - T_0}\right)^2 - \left(\frac{1}{800 - T_0}\right)^2\right] \cdot F_2 \tag{1}$$

E = heat input (kJ/mm),
T_0 = working temperature (°C),
k = thermal efficiency,
d = material thickness (mm),
F_2 = joint type factor (for butt joints the value is 0.9),

The component "**E**" of the above equation is originally defined as an Arc Energy in kJ/mm (theoretical heat input), but it was replaced by the Energy of laser beam defined as a quotient of the laser power and welding speed: E = W/v (kJ/mm). In turn the thermal efficiency "**k**" is given for different arc processes and indicates the amount of heat really transferred into the material. Adopting the **k** factor for laser welding conditions, it was assumed that the thermal efficiency is directly correlated to the value of laser beam absorption by the material. Thus in the case of conduction laser welding mode the laser beam energy is absorbed on the top surface of a joint and a weld pool (so-called Fresnel absorption). Value of the Fresnel absorption for a diode laser radiation with a wavelength of 808 nm on the surface of steel is 0.6, so this value was taken as the thermal efficiency "**k**". The working temperature was assumed as 20°C. The value of cooling time between 800 and 500°C during HPDDL laser welding of butt joints at heat input 380 J/mm is 7.2 s according to calculations, and about 6 to 8 s estimated by measurements on the top surface of joint. However, in the case of heat input of 380 J/mm the calculated cooling time reaches 22 s, compared to 19÷21 s estimated by measurements on the top surface, Table 4.

As shown on the Fig. 5,6. and in Table 4, the width of HAZ for the cooling time $t_{8/5}$ = 7.2 s (heat input 380 J/mm) is about 1.5 mm. Micrographs show clearly that the HAZ structure in the region adjacent to the BM is very fine grained, with the average grain size in this region about 5÷7 μm, Fig. 6. In turn, from the fusion line grain growth region can be observed (coarse-grain structure), with grain size up to 43 μm, Fig. 6.

Moreover, a transitional region may be observed in the HAZ, Fig. 6. HAZ structure of the butt joint produced at maximum heat input of 660 J/mm and cooling time $t_{8/5}$ = 22.0 s is similar but the HAZ width is much greater about 2.5 mm, Table 4.

TABLE 4

Relationship between the heat input, HAZ width and cooling times $t_{8/5}$, for the butt joints of 2.5 mm thick S420MC steel sheets welded by the HPDDL laser beam

Joint no.	Heat input J/mm	HAZ width mm	cooling time $t_{8/5}$ (s)	
			measured*	calculated
A	380	1.5	6÷8	7.2
C	660	2.5	19÷21	22.0

Remarks: * – the value was estimated by pyrometer measurements on the top surface of welded joints in the area adjacent to the weld face
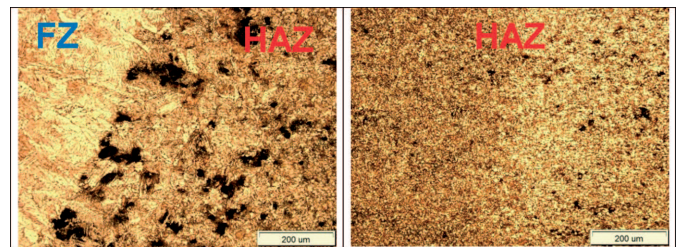

Fig. 6. HAZ microstructure of the butt joint produced by HPDDL at 380 J/mm; FZ – fusion zone, HAZ – heat affected zone

Microhardness profiles measured for all test joints were very similar. The measurements, conducted on the cross-sections of butt joints, showed just a slight increase of microhardness in the fine-grained HAZ to about 220 HV0.2, compared to the microhardness of base material (BM) about 170÷180 HV0.2, and next fall of microhardness to about 170 HV0.2 in the region of weld metal (fusion zone) composed of ferrite, Fig. 7.
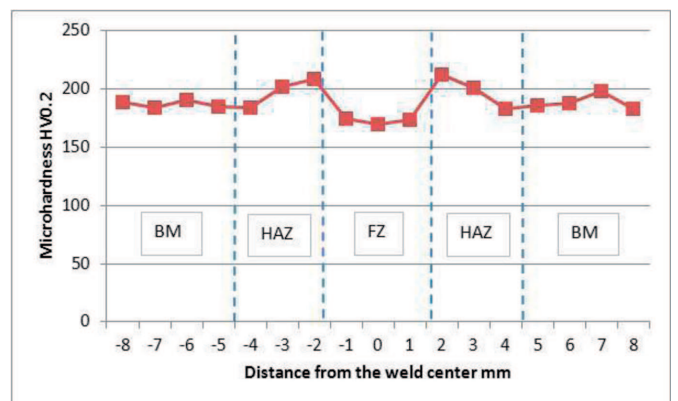

Fig. 7. Microhardness distribution on the cross-section of butt joint welded by the HPDDL at heat input of 660 J/mm, ($t_{8/5}$ = 22 s), Table 3,4

Mechanical tests and examinations have confirmed high mechanical performance of the test joints of S420MC steel welded by the HPDDL laser. The bending angle of all tested

TABLE 5

Parameters of butt joints welding of the 2.5 mm thick S420MC steel sheets using the Disk laser, Fig. 1,3,4,8,9

Test joint type	Laser power W	Welding speed mm/min	Heat input J/mm	Width of the weld face mm	Width of the weld root mm	Bend angle °	Tensile strength MPa
A	2200	3000	44	0.9	0.8	180	576
B	2200	3500	38	0.7	0.7	180	571

Remarks: other parameters of laser welding: wave length of laser radiation: 1030 nm, focusing lens focal length: 200 mm, collimator focal length: 200 mm, laser beam divergence: <8.0 mm·mrad, fiber core diameter: 200 μm, beam spot diameter: 200 μm, diameter of the gas shielding nozzles: 10.0 mm, shielding gas: Ar (purity 99.999%), gas feed rate on the top surface (face of weld): 15.0 l/min and from root 3.0 l/min

joints during the technological bend test reached a maximum value of 180°, without any cracks on the weld face, as well as on the weld root, Table 3. The joints breaking tensile during static tensile test was in a range 560 MPa to 570 MPa, and all samples were broken in the BM, so tensile strength of test joints was not lower than the tensile strength of the S420MC steel, Table 3.

In order to compare the autogenous laser welding by HPDDL laser to Disk laser welding, additionally welding test of 2.5 mm thick butt joints of S420MC steel were performed by the Disk laser at laser power 2.2 kW (the same as in a case of HPDDL welding) and different welding speed.

It was found that the welding speed required for full penetration of the 2.5 mm thick butt joints of S420MC steel is ten times higher compared to the HPDDL laser welding, at the same laser power 2.2 kW. Thus the heat input of welding is just 38 J/mm. Macrograph of the butt joint welded at 38 J/mm by Disk laser shows that the fusion zone is in hourglass configuration (X shape), Fig. 3. The width of weld face as well as the root is very narrow just 0.7 mm, therefor the depth/width ratio of fusion zone is 3.6, Fig. 3, Table 5. The geometry of the fusion zone shows clearly that the mode of Disk laser welding was keyhole welding. Such a welding mode is the result of relatively high power density of the circular laser beam focused to a diameter of 200 μm. The power density of the laser beam spot at 2.2 kW reaches $7 \cdot 10^6$ W/cm^2, thus enough to form a keyhole during steel plate welding. Macrostructure observations reveled small single pores placed in a middle of the weld. The diameter of single pores was in a range 0.1÷0.15 mm. Due to very narrow weld face and very dynamic changes of temperatures in the keyhole region, measurement of the thermal cycle was not possible. Therefore the cooling time between 800 and 500°C ($t_{8/5}$) was estimated just analytically in the same way as for HPDDL welding, but the value of the thermal efficiency "**k**" was taken as 0.9 (equal to the laser beam absorption during keyhole welding mode). The calculated value of cooling time $t_{8/5}$ for heat input at 38 J/mm is just 0.16 s, so the average cooling rate under these conditions is very rapid and reaches value of about $1.9 \cdot 10^3$ Ks^{-1}.

Very rapid cooling rates during the Disk laser welding of butt joints have strong impact on the microstructure of FZ and HAZ, Fig. 8. The microstructure and grains orientation in the FZ indicate the cellular solidification mode of the weld pool, Fig. 8. The macrostructure, and also microstructure show columnar crystals arranged parallel to each other. It is obvious that crystals were rapidly growing from the vertical fusion line towards to the weld center, in the direction of fast heat flow, Fig. 8.

The microstructure of weld metal (FZ) produced at heat input of just 38 J/mm consists of polygonal ferrite (α_{pf}), allotriomorphic ferrite (α_{af}) and acicular ferrite (α_{ac}), Fig. 8. The widmanstatten ferrite was not identified in the FZ of Disk laser welded joints, in contrast to those produced by HPDDL welding, Fig. 8. The amount of acicular ferrite in the FZ of butt joint produced by Disk laser at 38 J/mm is about 35%, and the average grain size of polygonal ferrite is 10÷20 μm, so much smaller than in a case of HPDDL welding, Fig. 5,8. Width of the HAZ doesn't exceed 0.5 mm, Fig. 8. Although the HAZ is recrystallized, no distinct differences in grains size was observed, compared to base material, Fig. 4,8. Ferrite grain size in the HAZ region adjacent to the FZ boundary is in a range 10÷12μm, Fig. 8.
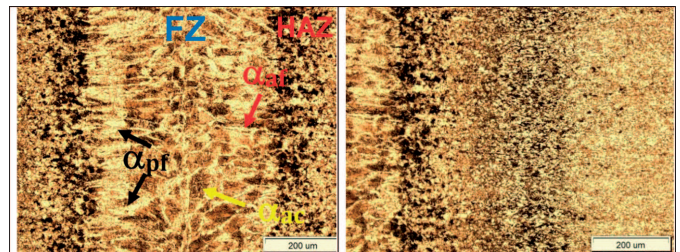

Fig. 8. Weld metal and HAZ microstructure of the butt joint produced by Disk laser at 38 J/mm

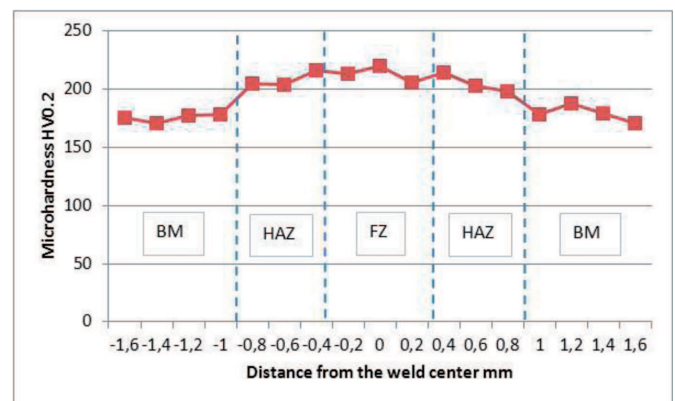Fig. 9. Microhardness distribution on the cross-section of butt joint welded by the Disk laser at heat input of 38 J/mm, ($t_{8/5}$ = 0.16 s), Table 5

Microhardness profiles measured for all test joints were very similar. Slight increase of microhardness in the fine-grained HAZ to about 220÷225 HV0.2 was observed, similarly like in a case of HPDDL welded joints, Fig. 9. While in the FZ microhardness remains at the same level about 210÷225 HV0.2, in contrast to the HPDDL welded joints. It may be explained by the differences in microstructures, especially distinct differences in grains size of the HPDDL and Disk laser welded joints.

Mechanical tests and examinations also have confirmed high mechanical performance of the test joints welded by the Disk laser. The bending angle of all tested joints was 180°, without any cracks. The average joints breaking tensile during static tensile test was over 570 MPa, and all samples were broken in the BM, similarly like in a case of joints welded by the HPDDL, Table 3,5.

4. Conclusions

Both lasers used in the study for autogenous welding allow to produce high quality butt joints of the S420MC steel sheets 2.5 mm thick, but the modes of welding are different, and thereby the conditions of solidification, cooling rates and structures are different.

The HPDOL laser produces good welds with flat and even surface, without undercuts and internal defect. However, due to relatively low power density $3.25 \cdot 10^4$ W/cm^2, the HPDOL allows just for conduction welding mode at heat input in the range of 380 to 660 J/mm, similarly like in a case of arc welding processes. The structure, fraction of acicular ferrite and grain size is clearly dependent on the heat input. The estimated cooling times $t_{8/5}$ from 7.2 to 22.0 s are rather typical for arc welding processes, therefore the widmanstatten ferrite was identified in the weld metal of all tested joints. Additionally weld metal of the joint produced at lowest heat input 380 J/mm contains about 25% of acicular ferrite, and low amount of polygonal ferrite with average grain size of 20÷30 μm, Fig. 5. In turn, the weld metal produced at 660 J/mm contains just about 15% of acicular ferrite, and also the grain size of polygonal ferrite is increase to 52 μm.

Due to very high power density of the Disk laser beam of $7 \cdot 10^6$ W/cm^2, the butt joints were welded at keyhole mode. The welding speed required for full penetration of the 2.5 mm thick butt joints was ten times higher, compared to the HPDL. So high welding speed resulted in very low heat input just 38 J/mm, for which the calculated value of cooling time $t_{8/5}$ is just 0.16 s, so the average cooling rate reaches is $1.9 \cdot 10^3$ Ks^{-1}. Such conditions favor the formation of very fine-grained structure with large fraction of acicular ferrite in the FZ and very narrow HAZ.

Acknowledgements

REFERENCES

[1] A. Lisiecki, Diode laser welding of high yield steel, Proc. of SPIE, Vol. 8703, Laser Technology 2012: Applications of Lasers, 223-234, 22 January 2013.

[2] J. Górka, Analysis of simulated welding thermal cycles S700MC using a thermal imaging camera, Adv. Mat. Res. ISI Proceedings 837, 375-380 (2014).

[3] K. Krasnowski, Influence of Stress Relief Annealing on Mechanical Properties and Fatigue Strength of Welded Joints of Thermo-Mechanically Rolled Structural Steel Grade S420MC, Arch. Metall. Mater. 54, 1059-1072 (2009).

[4] Ming Gao, Xiaoyan Zeng, Qianwu Hu, Jun Yan, Laser-TIG hybrid welding of ultra-fine grained steel, J. Mat. Proc. Tech. 209, 785-791 (2009).

[5] Rajashekhar S. Sharma, Pal Molian, Weldability of advanced high strength steels using an Yb:YAG disk laser, J. Mat. Proc. Tech. 211, 1888-1897 (2011).

[6] J. Górka, Influence of the maximum temperature of the thermal cycle on the properties and structure of the HAZ of steel S700MC, IOSR J. of Eng. 3, (11), 22-28 (2013).

[7] J. Bodzenta, A. Kaźmierczak, T. Kruczek, Analysis of thermograms based on FFT algorithm, J. de Physique IV 129, 201-206 (2004).

[8] A. Klimpel, A. Lisiecki, A. Szymanski, A.P. Hoult, Numerical and experimental determination of weld pool shape during high-power diode laser welding, Proc. of SPIE 5229, Laser Technology VII: Applications of Lasers, 6 Oct. 2003, 247-250, doi:10.1117/12.520726.

[9] A. Kurc-Lisiecka, W. Ozgowicz, W. Ratuszek, J. Kowalska, Analysis of Deformation Texture in AISI 304 Steel Sheets, Sol. St. Phenomena 203-204, 105-110 (2013).

[10] W. Sitek, L.A. Dobrzański, Comparison of hardenability calculation methods of the heat-treatable constructional steels, J. Mat. Proc. Tech. 64, (1-3), 117-126 (1995).

[11] W. Sitek, J. Trzaska, L.A. Dobrzański, Modified Tartagli method for calculation of Jominy hardenability curve, Mat. Sci. Forum 575-578, 892-897 (2008).

[12] K. Janerka, D. Bartocha, J. Szajnar, J. Jezierski, The carburizer influence on the crystallization process and the microstructure of synthetic cast iron, Arch. Metall. Mater. 55, (3), 851-859 (2010).

[13] L.A. Dobrzański, A. Grajcar, W. Borek, Microstructure evolution of C-Mn-Si-Al-Nb high-manganese steel during the thermomechanical processing, Mat. Sci. Forum 638, 3224-3229 (2010).

[14] M. Opiela, A. Grajcar, Hot deformation behavior and softening kinetics of Ti-V-B microalloyed steels, Arch. Civ. Mech. Eng. 12, (3), 327-333 (2012).

[15] R. Burdzik, Ł. Konieczny, Research on structure, propagation and exposure to general vibration in passenger car for different damping parameters, J. of Vibroengineering 15, (4), 1680-1688 (2013).

[16] T. Wegrzyn, J. Piwnik, D. Hadrys, Oxygen in Steel WMD after Welding with micro-jet cooling, Arch. Metall. Mater. 58, (4) 1067-1070 (2013).

[17] T. Wegrzyn, J. Piwnik, R. Wieszała, D. Hadryś, Control over the steel welding structure parameters by micro-jet cooling, Arch. Metall. Mater. 57, (3) 679-685 (2012).

[18] T. Wegrzyn, J. Piwnik, Low alloy steel welding with micro-jet cooling, Arch. Metall. Mater. 57, (2) 539-543 (2012).

[19] A. Kazmierczak-Balata et al., Determination of thermal, elastic, optical and lattice parameters of GdCOB single crystals doped with Nd3+ and Yb3+ ions, J. of Alloys and Comp. 481, (1-2), 622-627 (2009).

[20] L.A. D o b r z a ń s k i, M. B o n e k, M. P i e c, E. J o n d a, Diode laser modification of surface gradient layer properties of a hot-work tool steel, Mat. Sci. Forum **(532-533)**, 657-660 (2006).

[21] D. J a n i c k i, Fiber laser welding of nickel based superalloy Rene 77, Proc. SPIE, Laser Technology 2012: Applications of Lasers, 2013, **8703**, 87030Q, doi: 10.1117/12.2013428.

[22] D. J a n i c k i, Fiber laser welding of nickel based superalloy Inconel 625, Proc. SPIE, Laser Technology 2012: Applications of Lasers, 2013, **8703**, 87030R, doi: 10.1117/12.2013430.

[23] A. L i s i e c k i, Welding of titanium alloy by Disk laser. Proc. of SPIE Vol. 8703, Laser Technology 2012: Applications of Lasers, 87030T (January 22, 2013); doi:10.1117/12.2013431.

[24] M. M u s z t y f a g a, L.A. D o b r z a ń s k i, S. R u s z, M. S t a s z u k, Application examples for the different measure-ment modes of electrical properties of the solar cells, Arch. Metall. Mater. **59**, (1) 247-252 (2014).

[25] A. G r a j c a r, M. R ó ż a ń s k i, S. S t a n o, A. K o w a l - s k i, B. G r z e g o r c z y k, Effect of Heat Input on Mi-crostructure and Hardness Distribution of Laser Welded Si-Al TRIP-Type Steel, Adv. in Mat. Sci. and Eng. **2014** (2014), Art. ID 658947, http://dx.doi.org/10.1155/2014/658947.

[26] J. S l a n i a, B. S l a z a k, M. F i d a l i, Application of fast fourier transform (FFT) in the analysis of a welding current instantaneous values waveforms during welding with a covered electrode, Arch. Metall. Mater. **59**(2), 569-573 (2014).

[27] R. B u r d z i k, Ł. K o n i e c z n y, Z. S t a n i k, P. F o l e g a, A. S m a l c e r z, A. L i s i e c k i, Analysis of impactof chosen parameters on the wear of camshaft, Arch. Metall. Mater. **59**(3), 961-967 (2014).